Chemical Engineering Journal 446 (2022) 137087

Contents lists available at ScienceDirect

Chemical Engineering Journal

journal homepage: www.elsevier.com/locate/cej

Subnanometer Single-Walled carbon nanotube growth from Fe-Containing Layered double hydroxides

Shulan Hao [a], Liu Qian [b], Qianru Wu [a], Dong Li [a], Fangqian Han [a], Lihu Feng [a], Liantao Xin [a], Tao Yang [c], Shiying Wang [a], Jin Zhang [b], Maoshuai He [a,*]

[a] College of Chemistry and Molecular Engineering, Qingdao University of Science and Technology, Qingdao 266042, China
[b] Center for Nanochemistry, Beijing Science and Engineering Center for Nanocarbons, Beijing National Laboratory for Molecular Sciences, College of Chemistry and Molecular Engineering, Peking University, Beijing 100871, China
[c] School of Environmental and Chemical Engineering, Jiangsu Ocean University, Lianyungang, 222005, Jiangsu, China

ARTICLE INFO

Keywords:
Single-Walled Carbon Nanotubes
Layered Double Hydroxide
Synergistic Effect
Selective Growth

ABSTRACT

High-quality single-walled carbon nanotubes (SWNTs) were synthesized on layered double hydroxides (LDHs) containing Fe and FeCo by CO chemical vapor deposition (CVD). Systematic investigations were performed to study the effects of temperature and catalyst composition on the diameter and chirality distributions of SWNTs. It was revealed that both catalysts produced subnanometer SWNTs at low reaction temperatures, correlated with the catalyst performances and reaction parameters. Particularly, SWNTs with enriched (6, 5) species were synthesized at 600 °C from LDHs containing bimetallic FeCo. Besides, the SWNT chirality distribution was further narrowed by a two-phase extraction method and the extracted (6, 5) SWNTs occupy about 57% of all semiconducting species. This work extends the development of robust LDH-based catalysts for chirality-selective synthesis of SWNTs, which paves the way to large scale production of subnanometer SWNTs for potential applications in electronics and optoelectronics.

1. Introduction

Since the landmark work of Iijima in the 1990s [1], carbon nanotubes have been the focus of extensive research in various fields. Particularly, single-walled carbon nanotubes (SWNTs) exhibit fascinating optical and electrical properties owing to their unique structure and high aspect ratio [2,3]. These properties are correlated with the chirality structures of SWNTs, which are denoted by chiral index (n, m) [4]. To realize their cutting-edge applications [5,6], it is necessary to obtain SWNTs with a narrow chirality distribution. Although various post-growth sorting techniques have been developed to separate SWNTs according to their conductivities or even chiralities [7,8], these processes usually suffer high cost and low yield. As a result, directly growing SWNTs with specific structures by chemical vapor deposition (CVD) method [9], also named as selective growth, arises as a promising approach for achieving single-chirality SWNTs [10].

During CVD growth process, the catalyst is of great importance in regulating both the SWNT nucleation thermodynamics and growth kinetics [11,12], ultimately affecting the SWNT chirality distribution. Compared with the large variety of catalysts which offer SWNT growth on flat substrate [11,13–15], the types of solid supported catalysts are fewer and mainly Fe-family based catalysts have been proven to be active for efficiently growing SWNTs with the potential to scale up [16–18]. Pioneer work in designing solid supported catalyst was reported by Resasco's group [16]. The silica supported CoMo catalyst affords the synthesis of SWNTs with major (6, 5) and (7, 6) species. Later, other catalyst systems, including FeCo/zeolite [19], Co/MCM-41[20], FeCu/MgO [21], $Co_xMg_{1-x}O$ [17], FeRu/SiO_2 [22] were also reported to be efficient in growing small diameter SWNTs with narrow chirality distributions. Among them, oxide solid solutions demonstrate the advantages of high metal dispersion and forming metal particles having strong interaction with the underlying support [17,23], favoring the generation of uniform nanoparticles for catalyzing structurally identical SWNTs. Layered double hydroxides (LDHs) represent a class of synthetic anionic clays containing charged brucite-like layers of divalent and trivalent metal [24], the excessive charge of which is balanced by anions in the interlayer. Owing to the specific structures, LDHs exhibit excellent expanding properties, highly flexible composition, and versatile

* Corresponding author.
E-mail address: hemaoshuai@qust.edu.cn (M. He).

https://doi.org/10.1016/j.cej.2022.137087

Available online 19 May 2022

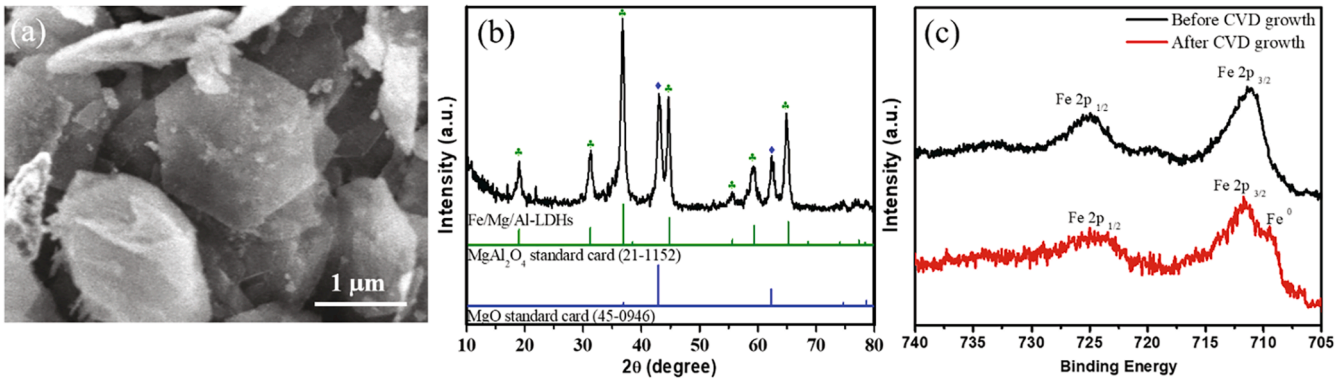

Fig. 1. (a) SEM image and (b) XRD pattern of Fe/Mg/Al LDHs. (c) XPS spectra of Fe 2p of Fe/Mg/Al LDHs before and after CVD growth at 800 °C.

physical and chemical properties correlated with a variety of host–guest assemblies. Besides, LDHs are readily synthesized by a simple protocol like co-precipitation. In terms of application in the heterogeneous catalysis, LDHs offer a number of advantages: Firstly, LDHs demonstrate a high adsorption capacity, which makes them effective supports for immobilizing catalytically active species on the surface even after thermal treatment; Secondly, metal cations are uniformly distributed at the atomic level in the layers, and tend to form uniform metal particles upon reduction, providing the possibility of high catalytic activity and selectivity. Thirdly, the tunable basicity of the surface enables LDHs and mixed metal oxides to perform as excellent solid base catalysts [24]. Consequently, LDHs have been applied as catalysts for growing carbon nanotubes since the 2000s [25]. Early works using either binary or ternary LDHs which have active Co or Fe components only led to the formation of multi-walled carbon nanotubes or carbon fibers [26–28]. Using mixed $Fe_{0.1}Mg_2Al_{0.9}$ oxides prepared from LDH calcination, Zhao et al. realized the synthesis of SWNTs although the nanotube quality and purity were not high [27]. By finely tuning the catalyst performances of LDHs and the CVD growth conditions, Wei's group reported the growth of a composite of single/double-walled carbon nanotubes interlinked with LDH flakes [29,30]. Later, short aligned SWNTs arrays were prepared from perpendicular Mo-containing Fe/Mg/Al LDH by CH_4 CVD [31]. However, due to the large diameters of active particles formed during reaction process, the synthesized large-diameter SWNTs have a wide diameter distribution [30]. As a result, it is still challenging to synthesize SWNTs with a narrow chirality distribution from LDH catalysts.

To fill the research gap, we herein prepared Fe/Mg/Al and Co/Fe/Mg/Al LDHs for catalytic synthesis of SWNTs by CO CVD. The catalytic performances of LDHs are sensitive to the calcination conditions, which is coherently related to the metal-support interactions in heterogeneous catalysis. Systematic characterizations on the prepared SWNTs reveal that subnanometer SWNTs are synthesized on monometallic Fe/Mg/Al LDH at a reaction temperature of 700 °C, the lowest activation temperature of the catalyst. By incorporating Co into the Fe/Mg/Al LDHs, the lowest SWNT growth temperature decreased to 600 °C, favoring the preferential synthesis of (6, 5) tubes. (6, 5) SWNT concentration could be further enriched by a two-phase extraction approach. This work not only extends the application of LDHs as robust catalysts for chiral-selective growth of SWNTs, but also deepens the understandings of SWNT nucleation mechanisms from LDHs.

2. Material and methods

2.1. Preparation of Fe/Mg/Al and Co/Fe/Mg/Al LDHs.

The Fe/Mg/Al flakes were prepared by a well-established co-precipitation technique [29]. The precursors for each composition are Fe $(NO_3)_3{\cdot}9H_2O$, $Mg(NO_3)_2{\cdot}6H_2O$ and $Al(NO_3)_3{\cdot}9H_2O$, respectively. The initial molar ratio of Fe, Mg and Al was 0.2:2:1. Urea with a concentration of 3.0 mol/L was applied to tune the pH value of the solution. After refluxing at 100 °C for 12 h, the suspension was kept at 95 °C for another 12 h. The produced Fe/Al/Mg LDHs were further filtered, rinsed, freeze-dried and finally annealed at 1000 °C for 6 h under ambient atmosphere. A similar procedure was adopted for preparing Co/Fe/Al/Mg LDHs, except that $Co(NO_3)_2{\cdot}6H_2O$ with an equivalent molar amount as that of $Fe(NO_3)_3{\cdot}9H_2O$ was added in the solution. The molar ratio of Co, Fe, Mg and Al in Co/Fe/Al/Mg LDHs was 0.2:0.2:2:1.

2.2. CVD growth of carbon nanotubes.

Ambient pressure CVD was carried out in a horizontal reaction with a quartz tube (inner diameter: 40 mm) [32,33]. The LDH catalyst was placed in a ceramic boat and loaded into the center of the reactor. After flushing with Ar, the system was increased to desired temperature in 300 sccm Ar. Once reaching the targeted temperature, Ar was replaced by 300 sccm CO and the reaction lasted 35 min. The reactor was finally cooled in 300 sccm Ar atmosphere. The system was kept at ambient pressure throughout the reaction process.

2.3. Characterizations of catalysts and carbon nanotubes.

The prepared LDH flakes were characterized by X-ray powder diffraction (XRD, D/MAX/2500PC) at ambient temperature. To monitor the composition evolution of the LDHs before and after CVD growth, X-ray photoelectron spectroscopy (XPS, Thermo Fisher ESCALAB 250 Xi) was performed with a Surface Science Instruments SSX-100 ESCA spectrometer. Scanning electron microscopy (SEM, Regulus 8100) was adopted to characterize the morphologies of the LDH flakes and carbon nanotubes. Raman spectroscopy (Renishaw inVia confocal), UV–vis-NIR absorption spectroscopy (Cary 5000) and photoluminescence (PL) spectroscopy (Horiba Jobin-Yvon NanoLog) were adopted to evaluate the diameter and chirality distribution of obtained SWNTs. Prior to absorption and PL spectroscopy characterizations, the SWNTs were purified and dispersed in aqueous sodium deoxycholate (2 wt%). Transmission electron microscopy (TEM, JEM-2100PLUS) was performed to investigate the structures of generated carbon nanotubes. Energy-dispersive X-ray spectroscopy (EDS, Nidec EX-37001) element mapping was adopted to investigate the metal dispersion in the LDH catalysts.

2.4. Partition of SWNTs using an aqueous two-phase extraction method.

An aqueous two-phase method [34] was used to enrich (6, 5) tubes from SWNTs dispersed in aqueous sodium deoxycholate (0.5 wt%). A mixture containing 2.15 ml SWNTs, 4.25 ml H_2O and 40.8 ml STOCK-A was first centrifuged at 8000 r/min for 5 min. The bottom phase of first step and the same volume of STOCK-B were centrifuged at 1500 r/min

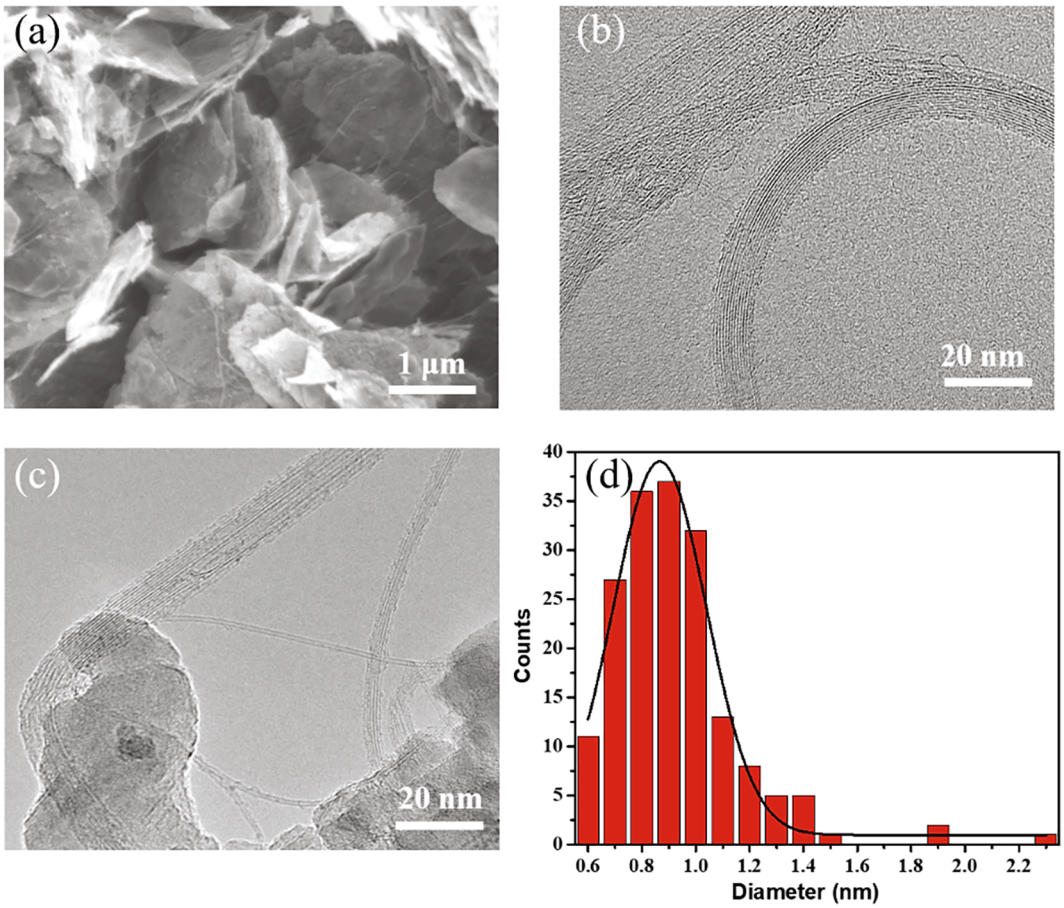

Fig. 2. (a) SEM image of the SWNTs grown on Fe/Mg/Al LDH catalyst at 800 °C. (b) and (c) TEM images of the SWNTs grown on Fe/Mg/Al LDH catalyst at 700 °C. (d) Diameter statistics of the SWNTs grown on Fe/Mg/Al LDH catalyst at 700 °C.

for 5 min. The bottom phase of the solution was further centrifuged with a same volume of STOCK-B. The bottom phase was subjected to UV–vis-NIR absorption and PL spectroscopy characterizations.

Specifically, STOCK-A solution contains: 14.1 g polyethylene glycol (PEG), 4.9 g dextran, 0.49 g sodium cholate, 1.117 g sodium dodecyl sulfate (SDS), 0.142 g NaCl and 100 g of H_2O; STOCK-B solution contains: 2.33 g dextran, 14.5 g PEG, 0.0473 g sodium deoxycholate, 1.8 g SDS and 100 g H_2O.

3. Results and discussion

Fig. 1**a** presents an SEM image of Fe/Mg/Al LDHs after calcination at 1000 °C. As reported previously [30,33], synthesized Fe/Mg/Al flakes exhibit typical hexagonal morphology. Such a plate morphology is mostly maintained even after thermal treatment. However, the chemical composition changes and the high temperature annealing transforms the LDHs into mixed solid oxide solution [26]. Indeed, XRD pattern (Fig. 1**b**) of the calcined LDHs exhibits characteristic reflections corresponding to crystalline phases of MgO and spinel $MgAl_2O_4$. The lack of diffraction peaks of iron oxide suggests that Fe is well dispersed in the oxides and could form solid solution with the oxide supports. The elemental dispersion in the Fe/Mg/Al catalyst was verified by EDS elemental mapping. Supporting Information **Figure S1** presents the elemental mapping of the catalyst and the overlapped image. All the elements, including Fe, Mg, Al, and O, are well dispersed. The Fe chemical composition in calcined LDHs was ascertained by XPS. Fig. 1**c** (upper one) shows the Fe 2p XPS core level spectrum of the Fe/Mg/Al catalyst. The binding energy of ~ 711 eV and the presence of satellite feature [35] indicates that the Fe component in the catalyst can be ascribed as Fe_2O_3.

CVD growth of carbon nanotubes on the calcined Fe/Mg/Al LDHs was carried out at ambient pressure using CO as the carbon precursor. Fig. 2**a** shows an SEM image of carbon nanotubes grown on the Fe/Mg/Al flakes at 800 °C. Under reaction conditions, it is speculated that Fe ions could be reduced and migrate to the flake surfaces, forming metallic Fe nanoparticles for subsequent nucleation and growth of carbon nanotubes. The speculation is verified by XPS characterizations on the Fe/Mg/Al flakes after CVD growth (Fig. 1**c**), where the intensity of Fe 2p centered at ~ 709 eV, correlated with reduced Fe [35,36], increases. The structure of the generated Fe particle is further analyzed by TEM (Supporting Information **Figure S2**). Grounded on the fast Fourier transformation pattern of the particle, its structure can be well assigned as Fe_3C. As low reaction temperature favors the growth of small diameter SWNTs, products grown at 700 °C was systematically investigated by TEM (Fig. 2**b, 2c**). Almost all the nanotubes are single-walled and tend to form small bundles because of the strong van der Waals interactions between them. Fig. 2**d** shows the statistical distribution of the SWNT diameter. Obviously, most of the SWNTs have diameters in the range of 0.7–1.0 nm.

Some previous studies also reported the growth of SWNTs from LDH precursors [30,31]. For example, using CH_4 as the carbon source, SWNTs were grown from Fe nanoparticles formed at 900 °C by reducing Fe/Mo/Mg/Al LDHs [30]. The produced SWNTs exhibit a wide diameter distribution, caused by the relatively high reaction temperature and the use of CH_4 as the carbon precursor. On the one hand, a high reaction temperature could overcome the nucleation barriers of most SWNTs [37], causing the growth of SWNTs with all possible diameters and chiralities. After nucleation, the chirality distribution of the produced

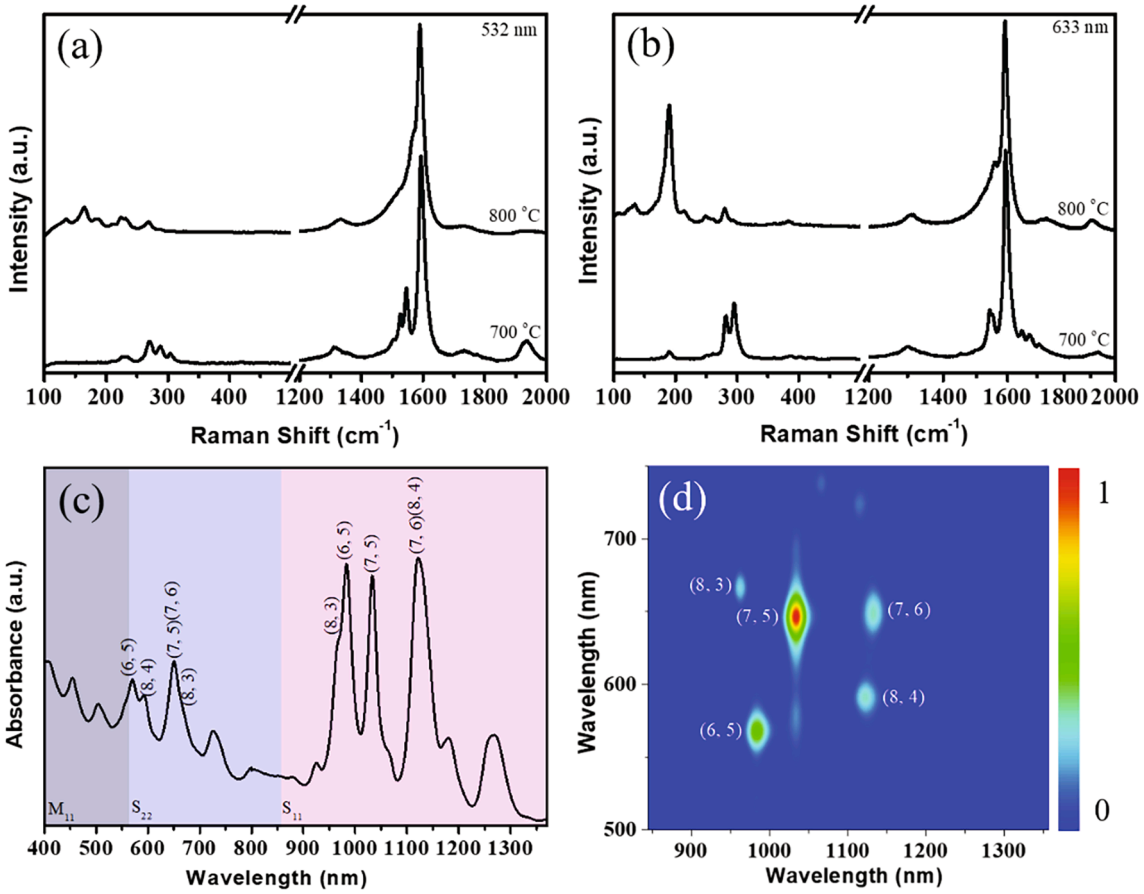

Fig. 3. (a) (b) Raman spectra of the as-obtained SWNTs on Fe/Mg/Al LDHs at 800 °C (upper one) and 700 °C (bottom one) using different excitation laser wavelengths. (c) Absorption spectrum and (d) normalized PL intensity map as a function of excitation and emission wavelength of 700 °C-grown SWNTs.

SWNTs is mainly determined by SWNT growth kinetics [38]. On the other hand, CH_4 tends to catalyze the SWNT growth by a tangential mode [39,40], where the diameter of nucleated SWNT is almost equal to that of catalyst particle. Later, hierarchical composites of carbon nanotubes interlinked LDH flakes were prepared with similar CVD parameters [30]. The carbon nanotubes also demonstrate a broad diameter distribution no matter what the wall numbers of the tubes were.

In order to minimize the SWNT diameter and chirality distribution, several strategies were adopted in our experiment. First, Fe/Mg/Al LDHs were calcined at a temperature as high as 1000 °C, which promotes the dissolution of Fe^{3+} inside the oxide matrix, forming atomically dispersed Fe in mixed solid solution. Under reducing atmosphere, only surface and subsurface Fe^{3+} are reduced, which subsequently migrate onto the support surface, and form small diameter Fe nanoparticles with uniform sizes. Indeed, XPS characterizations of the catalyst after CVD reaction confirmed the formation of reduced Fe (Fig. 1**c,** bottom one). Second, CO was applied as the carbon precursor during CVD process. It has been validated experimentally that CO favors the growth of small diameter SWNTs with a perpendicular mode [39] because of its high carbonization potential. Third, relatively low reaction temperatures were adopted in our CVD reaction process. Compared with a reaction temperature of 900 °C adopted in previous attempts [30,31], the reaction temperatures investigated in our work are generally lower than 800 °C. The low reaction temperature could only overcome the nucleation barriers and facilitate the growth of some small-diameter SWNT species. Grounded on the above analysis, we could expect that SWNTs grown on the calcined LDH catalysts might possess a narrow chirality distribution.

Optical characterizations were carried out to determine the diameter and chirality of SWNTs grown on calcined Fe/Mg/Al catalyst. Fig. 3**a and 3b** compare the Raman spectra of carbon nanotubes grown at 800 °C and 700 °C using two excitation laser wavelengths. The appearance of radial breathing modes (RBMs) and the high intensity ratio of G to D mode further confirm the production of high quality SWNTs. Besides, the relatively high RBM frequencies indicate the SWNTs possess small diameters. In particular, most of RBMs are located at frequencies larger than 250 cm^{-1}, suggesting that mainly subnanometer SWNTs are synthesized at 700 °C. In agreement with previous observations in other catalyst systems [18,22,41], SWNT chirality distribution becomes narrower as the CVD reaction temperature decreases. The major SWNT species grown on Fe/Al/Mg catalyst at 700 °C include (6, 5), (7, 5), (7, 6) and (8, 4) (Fig. 3**c**). The chirality distribution was crosschecked by PL map of the SWNT dispersion (Fig. 3**d**). Further decreasing the reaction temperature does not lead to the growth of SWNTs anymore (Supporting Information **Figure S3**). The failure in growing SWNTs at lower temperatures is correlated with the reductive properties of the monometallic Fe/Mg/Al catalyst. As addressed previously [3,42], SWNTs usually start to grow at a temperature higher than the threshold reduction temperature of the catalyst. Since iron oxide can only be reduced at temperatures higher than 700 °C [18,41], mainly trace amount of multi-walled carbon nanotubes are generated at 600 °C from the rare large diameter Fe nanoparticles. The large diameter iron oxide nanoparticles can be readily reduced and activated because they have very weak interactions with the oxide support.

In order to decrease the reduction temperature of Fe catalysts and narrow down the SWNT chirality distribution, a number of catalyst promoters, such as Cu [18], Mn [41], and Ru [22], were added into the Fe-based catalysts. In these bimetallic catalyst systems, the role of the second metal, which is easily reduced at low temperatures, is to promote the reduction of the iron oxide by a "spillover" mechanism, a phenomenon called as synergistic effect. As a result, low temperature SWNT

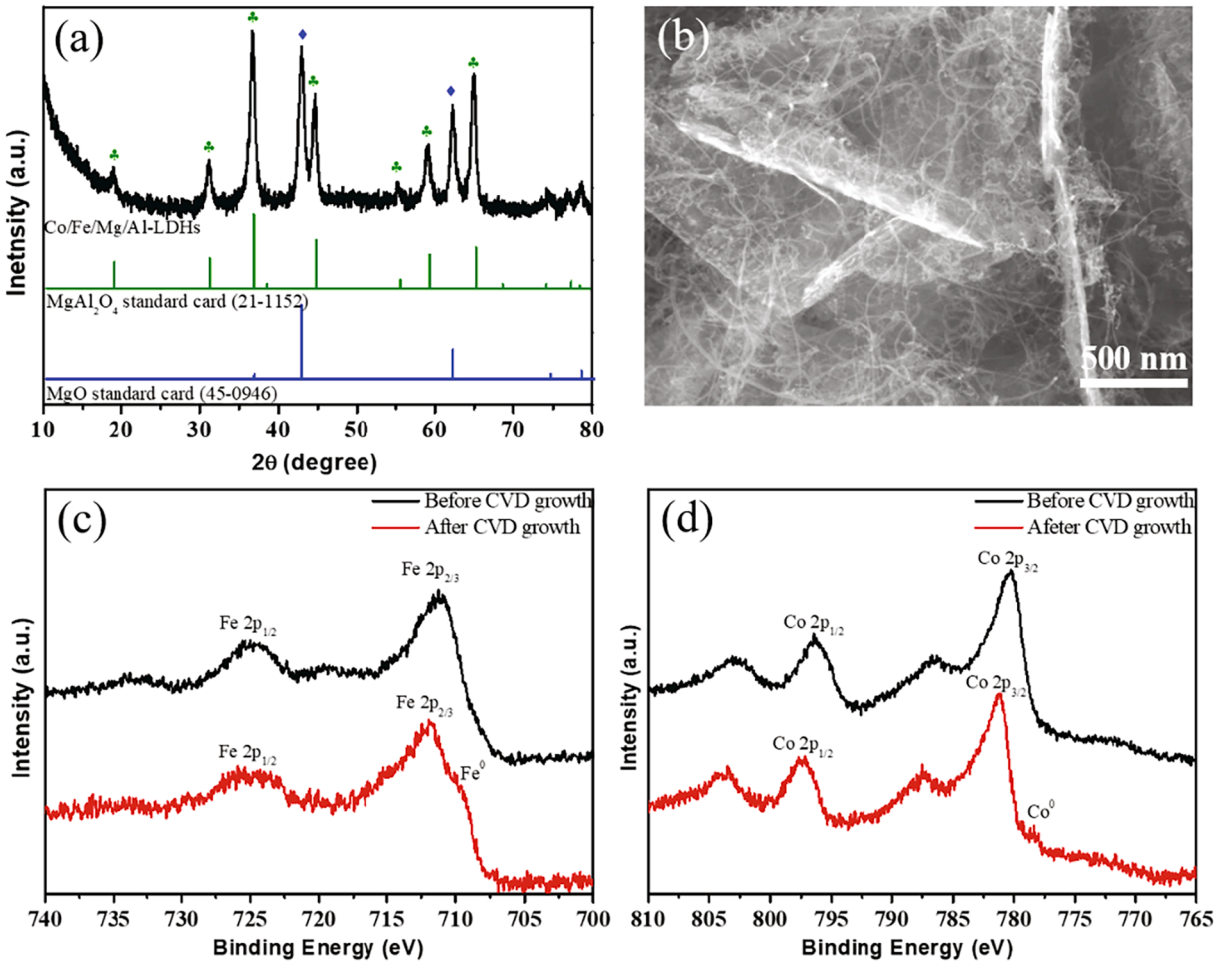

Fig. 4. (a) XRD pattern of Co/Fe/Mg/Al LDHs. (b) SEM image of carbon nanotubes grown from Co/Fe/Mg/Al LDHs at 800 °C. (c) XPS spectra of Fe 2p and (d) Co 2p of Co/Fe/Mg/Al LDHs before and after an 800 °C CVD process.

growth was achieved on the bimetallic SWNTs and the SWNTs generally demonstrate a narrow chirality distribution [18,22,41]. It is noted that in the bimetallic catalysts, the active component remains Fe, and the promoter metals themselves do not directly catalyze the nucleation of the SWNTs [43]. Alternatively, FeCo bimetallic catalysts have been proposed to efficiently grow carbon nanotubes [19,36]. For instance, Hardeman et al. observe a synergistic effect in active-active FeCo catalyst for growing thick carbon nanotube forest [36]. Maruyama's group developed a zeolite supported FeCo catalyst for growing high purity SWNTs using ethanol CVD [19]. Inspired by the works, we prepared bimetallic Co/Fe/Mg/Al flakes for catalyzing SWNTs growth. Prior to the CVD growth, the LDH flakes were calcined at 1000 °C to enhance their catalytic performances for growing SWNTs.

Fig. 4**a** presents the XRD profile of the calcined Co/Fe/Mg/Al catalyst. Similar to Fe/Mg/Al flakes (Fig. 1**b**, Supporting Information **Figure S4**), only diffraction peaks corresponding to MgO and $MgAl_2O_4$ were observed, indicating that both Fe and Co are well dispersed in the support matrix. Elemental map (Supporting Information **Figure S5**) further confirm that Fe and Co are well dispersed in the LDH catalyst. The Co/Fe/Mg/Al catalyst is also active for growing carbon nanotubes.

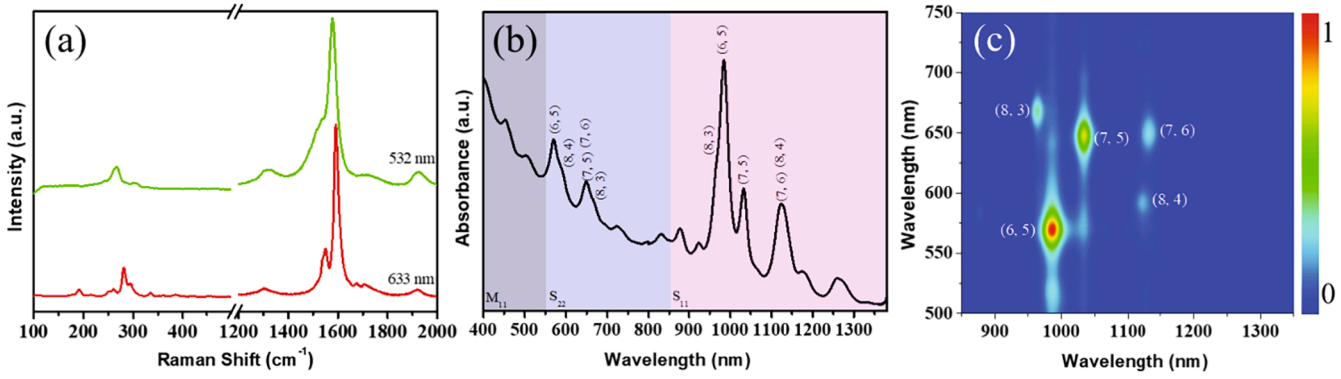

Fig. 5. (a) Raman spectra of the SWNTs grown on Co/Fe/Mg/Al LDHs at 600 °C. (b) Absorption spectrum and (c) normalized PL intensity as a function of excitation and emission wavelength of 600 °C-grown SWNTs.

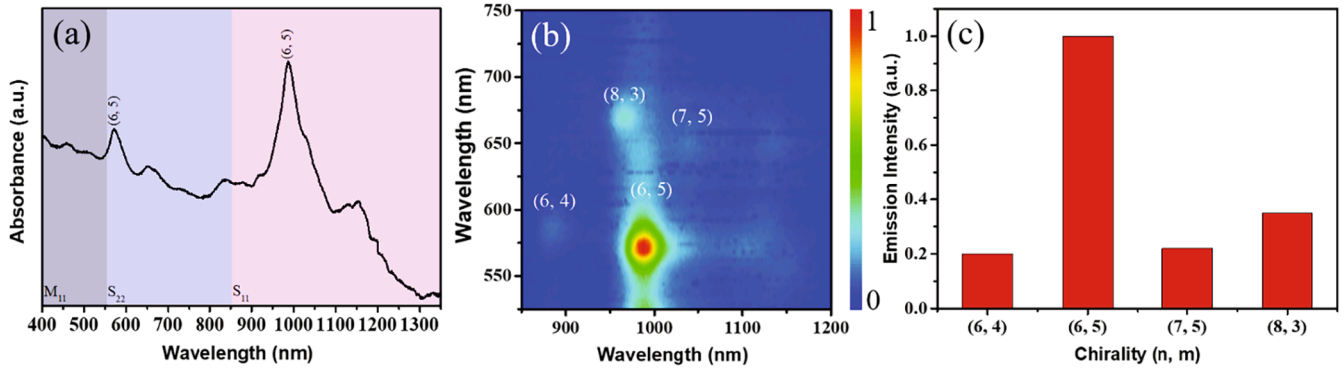

Fig. 6. (a) Absorption spectrum, (b) normalized PL intensity map and (c) PL intensity ratios of the SWNTs treated by aqueous two-phase extraction.

Fig. 4**b** shows a typical SEM image of carbon nanotubes grown at 800 °C, the nanotube density is much higher than that grown from Fe/Mg/Al catalyst (Fig. 2**a,** Fig. 4**b**), indicative of the synergistic effect in the Co/Fe/Mg/Al catalyst. In order to understand the carbon nanotube growth from the Co/Fe/Mg/Al LDH catalyst, XPS characterizations were carried out on the LDHs before and immediately after the CVD growth process. XPS profile reveals that all the Fe atoms in the raw catalyst are in oxide state (Fig. 4**c** upper one), the binding energies of Fe $2p_{1/2}$ and Fe $2p_{3/2}$ are respectively located at ~ 725 eV and ~ 711 eV. A Co $2p_{3/2}$ peak centered at ~ 781 eV is indicative of cobalt oxide (Fig. 4**d** upper one). The participation of both Fe and Co in growing carbon nanotube was also verified from differences in the XPS spectra before and after CVD reaction (Fig. 4**c**&**4d**).

In addition, low temperature growth of SWNTs is possible for Co/Fe/Mg/Al catalyst. Fig. 5**a** presents the Raman spectra of 600 °C-grown product. Clearly, the high frequency of RBMs and the relatively low D mode intensity suggest the production of high quality, small diameter SWNTs. Supporting Information **Figure S6** show the zoomed RBMs and the SWNT chirality assignment according to Kataura plot. As Raman scattering is a resonant process, the RBM intensity mainly depends on the energy match between the excitation laser wavelength and inter-band transition energy of the SWNTs. Adsorption spectrum (Fig. 5**b**) and PL (Fig. 5**c**) map of SWNTs grown at 600 °C indicate that enrichment of (6, 5) SWNTs was achieved, revealing that calcined Co/Fe/Mg/Al LDHs are promising in chirality-selective growth of SWNTs. Assuming the PL emission intensity is roughly proportional to the abundance of each SWNT species, the concentration of (6, 5) SWNT is estimated to be 37% among all the detected semiconducting SWNTs. Such a chirality enrichment is an interplay between SWNT nucleation thermodynamics and growth kinetics. Compared with enrichment of (6, 5) SWNTs from some state of art solid catalysts, including FeCu [18], Fe-SiC [44], CoMoCAT [45], the concentration is not very high. Improvement in (6, 5) SWNT enrichment is anticipated by increasing the CVD reaction pressure, as previously reported by Wang et al. [46]. It is noted that at low reaction temperatures, the possibility of only reduced Co nanoparticle is activated in Co/Fe/Mg/Al LDHs for growing SWNTs cannot ruled out. Supporting Information **Figure S7** present the optical characterizations of SWNTs grown on monometallic Co/Mg/Al LDHs. Systematic investigations on the catalytic performances of LDHs with tunable compositions are being carried out in our lab.

The SWNT chirality distribution can be further narrowed by an aqueous two-phase extraction method [34]. Owing to the curvature-related intrinsic hydrophobicity of SWNTs, spontaneous partition of SWNTs occurred. Fig. 6**a** presents the absorption spectrum of the bottom phase, which is less hydrophobic than the top phase. Clearly, enrichment of small diameter with predominant (6, 5) species was observed. Owing to the overlaps of S_{11} of different SWNT species with similar diameters, it is challenging to estimate the (6, 5) SWNT concentration from the absorption spectrum. Consequently, PL spectroscopy characterizations were performed on the extracted SWNTs and the (6, 5) tube content was improved to ~ 57% (Fig. 6**b, 6c**). The concentrations of other SWNT species did not show striking increase. This work thus provides the possibility for producing subnanometer SWNTs with a very narrow chirality distribution. By combining post-growth assembly techniques, these SWNTs could be applied in electronic and optoelectronics devices.

4. Conclusion

In summary, chirality-selective synthesis of SWNTs was achieved on Fe-based LDHs. The growth of subnanometer SWNTs is attributed to the optimized LDH calcination conditions, low reaction temperature and perpendicular SWNT growth mode. Particularly, preferential growth of (6, 5) SWNTs was realized on a calcined Co/Fe/Mg/Al catalyst at 600 °C. The concentration of (6, 5) SWNTs was increased to about 57% using an aqueous two-phase extraction method. This work not only extends the applications of LDHs in catalyzing SWNT growth, but also provides useful insights into catalyst activation and SWNT nucleation, which would ultimately help the growth of SWNTs with narrowly distributed chirality distribution, paving the way towards applications where SWNTs with uniform structures are needed.

Declaration of Competing Interest

The authors declare that they have no known competing financial interests or personal relationships that could have appeared to influence the work reported in this paper.

Acknowledgements

This work was supported by the National Natural Science Foundation of China (51972184) and Key Basic Research Project of Shandong Province (ZR2019ZD49). Funding from Taishan Scholar Advantage and Characteristic Discipline Team of Eco Chemical Process and Technology is also acknowledged. Prof. Q. Liu and Mr. Y. Zhang acknowledged for their experimental support and useful discussion.

Appendix A. Supplementary data

Supplementary data to this article can be found online at https://doi.org/10.1016/j.cej.2022.137087.

References

[1] S. Iijima, Helical microtubules of graphitic carbon, Nature 354 (6348) (1991) 56–58.
[2] F. Yang, M. Wang, D. Zhang, J. Yang, M. Zheng, Y. Li, Chirality pure carbon nanotubes: Growth, sorting, and characterization, Chem. Rev. 120 (2020) 2693–2758.

[3] M. He, S. Zhang, J. Zhang, Horizontal single-walled carbon nanotube arrays: Controlled synthesis, characterizations, and applications, Chem. Rev. 120 (2020) 12592–12684.

[4] M.S. Dresselhaus, G. Dresselhaus, R. Saito, A. Jorio, Raman spectroscopy of carbon nanotubes, Phys. Rep. 409 (2) (2005) 47–99.

[5] L. Liu, J. Han, L. Xu, J. Zhou, C. Zhao, S. Ding, H. Shi, M. Xiao, L.I. Ding, Z.E. Ma, C. Jin, Z. Zhang, L.-M. Peng, Aligned, high-density semiconducting carbon nanotube arrays for high-performance electronics, Science 368 (6493) (2020) 850–856.

[6] M. Zhao, Y. Chen, K. Wang, Z. Zhang, J.K. Streit, J.A. Fagan, J. Tang, M. Zheng, C. Yang, Z. Zhu, W. Sun, DNA-directed nanofabrication of high-performance carbon nanotube field-effect transistors, Science 368 (6493) (2020) 878–881.

[7] M.S. Arnold, A.A. Green, J.F. Hulvat, S.I. Stupp, M.C. Hersam, Sorting carbon nanotubes by electronic structure using density differentiation, Nat. Nanotechnol. 1 (1) (2006) 60–65.

[8] D. Yang, L. Li, X. Wei, Y. Wang, W. Zhou, H. Kataura, S. Xie, H. Liu, Submilligram-scale separation of near-zigzag single-chirality carbon nanotubes by temperature controlling a binary surfactant system, Sci. Adv. 7 (2021) eabe0084.

[9] J.R. Sanchez-Valencia, T. Dienel, O. Gröning, I. Shorubalko, A. Mueller, M. Jansen, K. Amsharov, P. Ruffieux, R. Fasel, Controlled synthesis of single-chirality carbon nanotubes, Nature 512 (7512) (2014) 61–64.

[10] M. He, S. Zhang, Q. Wu, H. Xue, B. Xin, D. Wang, J. Zhang, Designing catalysts for chirality-selective synthesis of single-walled carbon nanotubes: Past success and future opportunity, Adv. Mater. 31 (2019) 1800805.

[11] S. Zhang, L. Kang, X. Wang, L. Tong, L. Yang, Z. Wang, K. Qi, S. Deng, Q. Li, X. Bai, F. Ding, J. Zhang, Arrays of horizontal carbon nanotubes of controlled chirality grown using designed catalysts, Nature 543 (7644) (2017) 234–238.

[12] F. Yang, X. Wang, D. Zhang, J. Yang, D.A. Luo, Z. Xu, J. Wei, J.-Q. Wang, Z. Xu, F. Peng, X. Li, R. Li, Y. Li, M. Li, X. Bai, F. Ding, Y. Li, Chirality-specific growth of single-walled carbon nanotubes on solid alloy catalysts, Nature 510 (7506) (2014) 522–524.

[13] M. He, H. Amara, H. Jiang, J. Hassinen, C. Bichara, R.H.A. Ras, J. Lehtonen, E. I. Kauppinen, A. Loiseau, Key roles of carbon solubility in single-walled carbon nanotube nucleation and growth, Nanoscale 7 (47) (2015) 20284–20289.

[14] S. Huang, Q. Cai, J. Chen, Y. Qian, L. Zhang, Metal-catalyst-free growth of single-walled carbon nanotubes on substrates, J. Am. Chem. Soc. 131 (6) (2009) 2094–2095.

[15] D. Yuan, L. Ding, H. Chu, Y. Feng, T.P. McNicholas, J. Liu, Horizontally aligned single-walled carbon nanotube on quartz from a large variety of metal catalysts, Nano Lett. 8 (8) (2008) 2576–2579.

[16] S.M. Bachilo, L. Balzano, J.E. Herrera, F. Pompeo, D.E. Resasco, R.B. Weisman, Narrow (n, m)-distribution of single-walled carbon nanotubes grown using a solid supported catalyst, J. Am. Chem. Soc. 125 (37) (2003) 11186–11187.

[17] M. He, D. Li, T. Yang, D. Shang, A.I. Chernov, P.V. Fedotov, E.D. Obraztsova, Q. Liu, H. Jiang, E. Kauppinen, A robust $Co_xMg_{1-x}O$ catalyst for predominantly growing (6, 5) single-walled carbon nanotubes, Carbon 153 (2019) 389–395.

[18] M. He, A.I. Chernov, P.V. Fedotov, E.D. Obraztsova, J. Sainio, E. Rikkinen, H. Jiang, Z. Zhu, Y. Tian, E.I. Kauppinen, M. Niemelä, A.O.I. Krause, Predominant (6, 5) single-walled carbon nanotube growth on a copper-promoted iron catalyst, J. Am. Chem. Soc. 132 (40) (2010) 13994–13996.

[19] S. Maruyama, Y. Miyauchi, Y. Murakami, S. Chiashi, Optical characterization of single-walled carbon nanotubes synthesized by catalytic decomposition of alcohol, New. J. Phys. 5 (2003) 149.

[20] Y. Chen, D. Ciuparu, S.Y. Lim, Y.H. Yang, G.L. Haller, L. Pfefferle, Synthesis of uniform diameter single-wall carbon nanotubes in Co-MCM-41: Effects of the catalyst prereduction and nanotube growth temperatures, J. Catal. 225 (2004) 453–465.

[21] M. He, Y. Wang, X. Zhang, H. Zhang, Y. Meng, D. Shang, H. Xue, D. Li, Z. Wu, Stability of iron-containing nanoparticles for selectively growing single-walled carbon nanotubes, Carbon 158 (2020) 795–801.

[22] X. Li, X. Tu, S. Zaric, K. Welsher, W.S. Seo, W. Zhao, H. Dai, Selective synthesis combined with chemical separation of single-walled carbon nanotubes for chirality selection, J. Am. Chem. Soc. 129 (51) (2007) 15770–15771.

[23] M. He, X. Wang, L. Zhang, Q. Wu, X. Song, A.I. Chernov, P.V. Fedotov, E. D. Obraztsova, J. Sainio, H. Jiang, Anchoring effect of Ni^{2+} in stabilizing reduced metallic particles for growing single-walled carbon nanotubes, Carbon 128 (2018) 249–256.

[24] J. Feng, Y. He, Y. Liu, Y. Du, D. Li, Supported catalysts based on layered double hydroxides for catalytic oxidation and hydrogenation: General functionality and promising application prospects, Chem. Soc. Rev. 44 (2015) 5291–5319.

[25] W. Yang, Y. Kim, P.K.T. Liu, M. Sahimi, T.T. Tsotsis, A study by in situ techniques of the thermal evolution of the structure of a Mg-Al-CO_3 layered double hydroxide, Chem. Eng. Sci. 57 (15) (2002) 2945–2953.

[26] F. Li, Q. Tan, D.G. Evans, X. Duan, Synthesis of carbon nanotubes using a novel catalyst derived from hydrotalcite-like Co-Al layered double hydroxide precursor, Catal. Lett. 99 (3-4) (2005) 151–156.

[27] Y. Zhao, Q. Jiao, C. Li, J.I. Liang, Catalytic synthesis of carbon nanostructures using layered double hydroxides as catalyst precursors, Carbon 45 (11) (2007) 2159–2163.

[28] X. Xiang, L. Zhang, H. Hima, F. Li, D. Evans, Co-based catalysts from Co/Fe/Al layered double hydroxides for preparation of carbon nanotubes, Appl. Clay. Sci. 42 (3-4) (2009) 405–409.

[29] Q. Zhang, M.Q. Zhao, D.M. Tang, F. Li, J.Q. Huang, B. Liu, W.C. Zhu, Y.H. Zhang, F. Wei, Carbon-nanotube-array double helices, Angew. Chem. 122 (21) (2010) 3724–3727.

[30] M.Q. Zhao, Q. Zhang, X.L. Jia, J.Q. Huang, Y.H. Zhang, F. Wei, Hierarchical composites of single/double-walled carbon nanotubes interlinked flakes from direct carbon deposition on layered double hydroxides, Adv. Funct. Mater. 20 (4) (2010) 677–685.

[31] M. Zhao, G. Tian, Q. Zhang, J. Huang, J. Nie, F. Wei, Preferential growth of short aligned, metallic-rich single-walled carbon nanotubes from perpendicular layered double hydroxide film, Nanoscale 4 (2012) 2470–2477.

[32] Q. Wu, H. Zhang, C. Ma, D. Li, L. Xin, X. Zhang, N. Zhao, M. He, SiO_2-promoted growth of single-walled carbon nanotubes on an alumina supported catalyst, Carbon 176 (2021) 367–373.

[33] B. Xin, W. Gao, Z. Ji, S. Zhang, L. Xin, L. Zhao, H. Xue, Q. Wu, L. Zhang, C. Liu, J. Zhang, M. He, Carbon fiber-promoted activation of catalyst for efficient growth of single-walled carbon nanotubes, Carbon 156 (2020) 410–415.

[34] N.K. Subbaiyan, S. Cambré, A.N.G. Parra-Vasquez, E.H. Hároz, S.K. Doorn, J. G. Duque, Role of surfactants and salt in aqueous two-phase separation of carbon nanotubes toward simple chirality isolation, ACS Nano. 8 (2) (2014) 1619–1628.

[35] D.D. Hawn, B.M. DeKoven, Deconvolution as a correction for photoelectron inelastic energy losses in the core level XPS spectra of iron oxides, Surf. Interface Anal. 10 (2-3) (1987) 63–74.

[36] D. Hardeman, S. Esconjauregui, R. Cartwright, S. Bhardwaj, L. D'Arsié, D. Oakes, J. Clark, C. Cepek, C. Ducati, J. Robertson, The synergistic effect in the Fe-Co bimetallic catalyst system for the growth of carbon nanotube forests, J. Appl. Phys. 117 (2015), 044308.

[37] Y. Magnin, H. Amara, F. Ducastelle, A. Loiseau, C. Bichara, Entropy-driven stability of chiral single-walled carbon nanotubes, Science 362 (6411) (2018) 212–215.

[38] M. He, X. Wang, S. Zhang, H. Jiang, F. Cavalca, H. Cui, J.B. Wagner, T.W. Hansen, E. Kauppinen, J. Zhang, F. Ding, Growth kinetics of single-walled carbon nanotubes with a (2n, n) chirality selection, Sci. Adv. 5 (12) (2019).

[39] M. He, Y. Magnin, H. Jiang, H. Amara, E.I. Kauppinen, A. Loiseau, C. Bichara, Growth modes and chiral selectivity of single-walled carbon nanotubes, Nanoscale 10 (14) (2018) 6744–6750.

[40] M. He, Y. Magnin, H. Amara, H. Jiang, H. Cui, F. Fossard, A. Castan, E. Kauppinen, A. Loiseau, C. Bichara, Linking growth mode to lengths of single-walled carbon nanotubes, Carbon 113 (2017) 231–236.

[41] M. He, P.V. Fedotov, A. Chernov, E.D. Obraztsova, H. Jiang, N.a. Wei, H. Cui, J. Sainio, W. Zhang, H. Jin, M. Karppinen, E.I. Kauppinen, A. Loiseau, Chiral-selective growth of single-walled carbon nanotubes on Fe-based catalysts using CO as carbon source, Carbon 108 (2016) 521–528.

[42] M. He, A.I. Chernov, E.D. Obraztsova, J. Sainio, E. Rikkinen, H. Jiang, Z. Zhu, A. Kaskela, A.G. Nasibulin, E.I. Kauppinen, M. Niemelä, O. Krause, Low temperature growth of SWNTs on a nickel catalyst by thermal chemical vapor deposition, Nano Res. 4 (4) (2011) 334–342.

[43] M. He, B. Liu, A.I. Chernov, E.D. Obraztsova, I. Kauppi, H. Jiang, I. Anoshkin, F. Cavalca, T.W. Hansen, J.B. Wagner, A.G. Nasibulin, E.I. Kauppinen, J. Linnekoski, M. Niemelä, J. Lehtonen, Growth mechanism of single-walled carbon nanotubes on iron-copper catalyst and chirality studies by electron diffraction, Chem. Mater. 24 (10) (2012) 1796–1801.

[44] F. Han, L. Qian, Q. Wu, D. Li, S. Hao, L. Feng, L. Xin, T. Yang, J. Zhang, M. He, Narrow-chirality distributed single-walled carbon nanotube synthesized from oxide promoted Fe-SiC catalyst, Carbon 191 (2022) 146–152.

[45] A. Jorio, A.P. Santos, H.B. Ribeiro, C. Fantini, M. Souza, J.P. Vieira, C.A. Furtado, J. Jiang, R. Saito, L. Balzano, D.E. Resasco, M.A. Pimenta, Quantifying carbon-nanotube species with resonance raman scattering, Phys. Rev. B 72 (2005), 075207.

[46] B.O. Wang, L.I. Wei, L.U. Yao, L.J. Li, Y. Yang, Y. Chen, Pressure-induced single-walled carbon nanotube (n, m) selectivity on Co-Mo catalysts, J. Phys. Chem. C 111 (40) (2007) 14612–14616.